



# Quick and accurate estimation of the elastic constants using the minimum image method

Konstantin V. Tretiakov\*, Krzysztof W. Wojciechowski

Institute of Molecular Physics, Polish Academy of Sciences, Smoluchowskiego 17/19, 60-179 Poznań, Poland

## ARTICLE INFO

### Article history:

Received 4 July 2014

Accepted 25 December 2014

Available online 3 January 2015

### Keywords:

Elastic constants

Minimum image method

Lennard-Jones potential

Monte Carlo method

## ABSTRACT

A method for determining the elastic properties using the minimum image method (MIM) is proposed and tested on a model system of particles interacting by the Lennard-Jones (LJ) potential. The elastic constants of the LJ system are determined in the thermodynamic limit,  $N \rightarrow \infty$ , using the Monte Carlo (MC) method in the NVT and NPT ensembles. The simulation results show that when determining the elastic constants, the contribution of long-range interactions cannot be ignored, because that would lead to erroneous results. In addition, the simulations have revealed that the inclusion of further interactions of each particle with all its minimum image neighbors even in case of small systems leads to results which are very close to the values of elastic constants in the thermodynamic limit. This enables one for a quick and accurate estimation of the elastic constants using very small samples.

© 2015 Published by Elsevier B.V.

## 1. Introduction

Knowledge of elastic properties of materials around us is important not only from the scientific point of view but also for practical applications. In solids, the elastic properties can be described by the elastic constants which determine the relationship between strain and stress. Research on the elastic constants is carried out at different levels from microscopic to macroscopic, using both the theoretical and experimental methods. A special place in the study of elastic properties is taken by computer simulations, which can relatively easily supply data in areas where the experiments are either difficult or even cannot be performed, e.g. at extreme temperatures or pressures, or can be used to analyze hypothetical models or materials with unusual properties. The pioneering simulation work by Squire, Holt, and Hoover [1] was related to Monte Carlo calculations of the elastic properties of solid argon using the Lennard-Jones interatomic pair potential:

$$\phi(r_{ij}) = 4\epsilon \left[ \left( \frac{\sigma}{r_{ij}} \right)^{12} - \left( \frac{\sigma}{r_{ij}} \right)^6 \right], \quad (1)$$

where  $\sigma$  is the particle diameter,  $\epsilon$  sets the energy scale, and  $r_{ij}$  is the distance between particles  $i$  and  $j$ . Since that time a number of simulation methods to calculate the elastic properties of atomic

systems were established [2–11]. In the current work a simple extension for basic methods of calculation of elastic constants is proposed and tested on Lennard-Jones system.

The LJ potential plays a significant role in the computer simulations, not only because of its simplicity and elegance, but mainly for the fact that it is a model potential which allows to describe some physical properties of noble gases and various properties of simple liquids [12]. It is also a reference potential used to test variety of new theories and computational methods [13]. Typically, new methods to calculate the elastic constants are tested on the system of particles interacting via LJ potential only between nearest neighbors [14,3,15,16,6,17,8,9] so called a nearest-neighbor Lennard-Jones (LJnn) potential. From the point of view of conducting simulation, it is a well defined and very comfortable model, because a researcher does not have to take into account the long-range interactions. However, in real systems one can rarely afford such a simplification. There are few works devoted to the calculations of elastic properties of the LJ system including the further neighborhood [1,18,19], because such simulations are much more time consuming than those taking into account only the nearest neighbors or those with some fixed length of truncation of the LJ potential. Many different simplifications of the LJ potential can be found in the literature, starting from the aforementioned LJnn model, by the systems, wherein the particles interact with some cut potential [20] until a cut and sifted potential [21]. The last one has the advantage in molecular dynamics (MD) simulations that there is no discontinuity in the potential or the force. It is not surprising that the system in each of these approximations will have different thermodynamic properties.

\* Corresponding author. Tel.: +48 618695276; fax: +48 618684524.

E-mail address: [kvt@ifmpan.poznan.pl](mailto:kvt@ifmpan.poznan.pl) (K.V. Tretiakov).

An accounting of the long-range interactions in computer simulations is usually quite expensive. For example, when considering the interactions of ions or dipoles one cannot avoid either counting the Ewald sum [22–24], or applying the particle–mesh method [25] or application of the method of minimal image [26,27]. However, to obtain correct results for the energy and pressure in the case of the LJ potential system, the long-range corrections are often used. The long-range or tail corrections are computed by following formulas:

$$U_{LRC}^* = \frac{8}{9} \pi \rho^* \left[ \left( \frac{\sigma}{r_c} \right)^9 - 3 \left( \frac{\sigma}{r_c} \right)^3 \right], \quad (2)$$

$$p_{LRC}^* = \frac{32}{9} \pi \rho^{*2} \left[ \left( \frac{\sigma}{r_c} \right)^9 - \frac{3}{2} \left( \frac{\sigma}{r_c} \right)^3 \right], \quad (3)$$

where  $U^* = U/\epsilon$  is the dimensionless energy,  $p^* = p\sigma^3/\epsilon$  is the dimensionless pressure,  $r_c$  is the cutoff radius of the LJ potential,  $\rho^* = (N/V)\sigma^3$  is the reduced density,  $N$  is the number of particles, and  $V$  is the volume of the system. In the case of the elastic constants the use of analogous corrections does not lead to correct results. So, the effect of long-range interactions cannot be neglected.

The aim of this work is twofold. First, a simple, efficient and fairly accurate method of determining the elastic properties is introduced, which correctly takes into account the long-range interactions. This method, using the convention of minimum images, has been tested in NVT and NPT ensembles. Second, the elastic constants of the system of particles interacting via LJ potential are determined in the limit  $N \rightarrow \infty$ .

## 2. Elastic constants and basic methods of their calculations

The elastic constants at a fixed temperature are defined as follows:

$$C_{\alpha\beta\gamma\tau} = \frac{1}{V} \left( \frac{\partial^2 F}{\partial \eta_{\alpha\beta} \partial \eta_{\gamma\tau}} \right)_{\eta=0}, \quad (4)$$

where  $F$  is the Helmholtz free energy,  $V$  is the volume of reference state,  $\eta$  is the strain tensor. In general, taking into account the symmetry of the strain tensor, the tensor of elastic moduli has 21 independent components [28], however, the crystal symmetry usually implies a significant reduction of their number. The face-centered cubic structure (only the crystal with such structure will be considered in this paper) has only three independent elastic constants, which – using the Voigt notation – can be written as follows:  $C_{1111} = C_{11}$ ,  $C_{1122} = C_{12}$ , and  $C_{1212} = C_{44}$ . The free energy change corresponding to a thermodynamically reversible elastic deformation of cubic crystals at zero pressure [28] has the form:

$$\begin{aligned} \frac{\Delta F}{V} = & \frac{1}{2} C_{11} (\eta_{xx}^2 + \eta_{yy}^2 + \eta_{zz}^2) \\ & + C_{12} (\eta_{xx}\eta_{yy} + \eta_{xx}\eta_{zz} + \eta_{yy}\eta_{zz}) \\ & + 2C_{44} (\eta_{xy}^2 + \eta_{xz}^2 + \eta_{yz}^2). \end{aligned} \quad (5)$$

### 2.1. Equilibrium fluctuation formula (NVT ensemble)

For a central force system, the elastic constants are determined from the analysis of the fluctuations in the positions of the particles in thermodynamic equilibrium using the fluctuation formulas [1,7]:

$$C_{\alpha\beta\gamma\tau} = \frac{1}{V} \left\langle \sum_{i<j} \frac{1}{r^2} \left( \phi'' - \frac{\phi'}{r} \right) \Delta x_{\alpha}^{ij} \Delta x_{\beta}^{ij} \Delta x_{\gamma}^{ij} \Delta x_{\tau}^{ij} \right\rangle$$

$$\begin{aligned} & - \frac{1}{VkT} \left\langle \left( \sum_{i<j} \frac{\phi'}{r} \Delta x_{\alpha}^{ij} \Delta x_{\beta}^{ij} - \left\langle \sum_{i<j} \frac{\phi'}{r} \Delta x_{\alpha}^{ij} \Delta x_{\beta}^{ij} \right\rangle \right) \right. \\ & \times \left. \left( \sum_{i<j} \frac{\phi'}{r} \Delta x_{\gamma}^{ij} \Delta x_{\tau}^{ij} - \left\langle \sum_{i<j} \frac{\phi'}{r} \Delta x_{\gamma}^{ij} \Delta x_{\tau}^{ij} \right\rangle \right) \right\rangle \\ & + \frac{NkT}{V} (\delta_{\alpha\gamma} \delta_{\beta\tau} + \delta_{\alpha\tau} \delta_{\beta\gamma}), \end{aligned} \quad (6)$$

where  $\phi$  is interatomic potential of interaction, the symbol  $\langle \dots \rangle$  designates configurational averages,  $\delta_{ij}$  is the Kronecker delta,  $\Delta x_{\alpha}^{ij} = x_{\alpha}(i) - x_{\alpha}(j)$ , and  $r = |\Delta x_{\alpha}^{ij}|^2$ . In the case of noncentral interactions, the situation is more complicated and other approaches have to be used, because in general it is impossible to express the elastic energy as a function of the strain tensor [7].

### 2.2. Strain fluctuation formula (NPT ensemble)

At constant pressure, it is convenient to use the free enthalpy (Gibbs free energy) expansion:

$$\begin{aligned} \frac{\Delta G}{V_p} = & \frac{1}{2} B_{11} (\eta_{xx}^2 + \eta_{yy}^2 + \eta_{zz}^2) \\ & + B_{12} (\eta_{xx}\eta_{yy} + \eta_{xx}\eta_{zz} + \eta_{yy}\eta_{zz}) \\ & + 2B_{44} (\eta_{xy}^2 + \eta_{xz}^2 + \eta_{yz}^2), \end{aligned} \quad (7)$$

where the volume  $V_p$  of the system corresponds to the equilibrium state at  $p$ . The elastic constants  $B_{ij}$  at pressure  $p$  are in the following relation with elastic constants at zero pressure  $C_{ij}$ :  $B_{11} = C_{11} - p$ ,  $B_{12} = C_{12} + p$ , and  $B_{44} = C_{44} - p$ . In this case, the strain fluctuation formula proposed by Parrinello–Rahman [2] and modified by Ray [4,5] is widely used:

$$B_{\alpha\beta\gamma\tau} = \frac{kT}{V_p} [\langle \eta_{\alpha\beta} \eta_{\gamma\tau} \rangle - \langle \eta_{\alpha\beta} \rangle \langle \eta_{\gamma\tau} \rangle]^{-1}. \quad (8)$$

Herein the strain tensor is defined as:

$$\eta_{\alpha\beta} = \frac{1}{2} \left( \langle \tilde{h}_{\alpha\gamma} \rangle^{-1} \tilde{h}_{\gamma\tau} h_{\tau\gamma} \langle h_{\gamma\beta} \rangle^{-1} - \delta_{\alpha\beta} \right), \quad (9)$$

where  $h$  is the matrix that describes the size and shape of the simulation box, matrix  $\langle h \rangle$  describes reference box,  $\tilde{h}$  is the transpose matrix, and  $\langle \tilde{h} \rangle^{-1}$  is the inverse of the transpose of  $\langle h \rangle$ . It is convenient to choose the matrices  $\langle h \rangle$  and  $h$  as symmetric. In this paper a modified version of the Parrinello–Rahman method was used [29,30].

## 3. Evaluation of the elastic constants using the minimum image method (MIM)

Since the contribution to the elastic constants from long-range interactions cannot be ignored or easily corrected using eqs. analogous to those applicable in the case of the system pressure or energy (2)–(3), a simple extension of the two mentioned above methods is proposed here. It bases on using the minimum image method (MIM) that was previously used for calculations of the energy and pressure in systems with long-range interactions [26,27].

### 3.1. Minimum image method in the NVT ensemble

The simulations in the canonical ensemble are performed by the standard (Metropolis) Monte Carlo scheme [31]. However the fluctuation formula (6) is applied not only for the particles in the simulation box, but also for their images. The calculations are performed not only for the  $i$ th particle with coordinates  $(x_i, y_i, z_i)$  but also for its 26 images, so are taken in account the particles with

following coordinates  $(x_i + kL, y_i + kL, z_i + kL)$  where  $k = -1, 0, 1$ . Thus, the elastic constants can be written as:

$$C_{\alpha\beta\gamma\tau} = C_{\alpha\beta\gamma\tau}^{\text{BOX}} + C_{\alpha\beta\gamma\tau}^{\text{MIM}}, \quad (10)$$

where  $C_{\alpha\beta\gamma\tau}^{\text{BOX}}$  is the contribution to the elastic constants derived directly from the particles inside the simulation box and  $C_{\alpha\beta\gamma\tau}^{\text{MIM}}$  is the contribution from their images. The contribution of images to the elastic constants can be, in fact, seen as a contribution from a ‘mean field’ exerted on the particle by other particles taken into account. Hence it takes into account the symmetry of the position of the particles (and the symmetry of studied crystal) better than just the standard approach without the minimum images. This allows fairly well approximation of the contribution of the long-range interaction to the elastic constants. In consequence, however, the effective linear size of the system under consideration is increased from  $L$  to  $3L$ .

### 3.2. Minimum image method in the NpT ensemble

In the NpT method, the elastic constants are calculated from fluctuations of the simulation box. The correct values of the elastic constants can be obtained only when the configuration space of the system under study is sampled correctly. Therefore, the potential energy should be calculated as accurately as possible. Using the minimum image method, the potential energy of the particle  $i$  can be expressed as

$$U_i = \sum_j \phi_{ij}^{\text{BOX}} + \sum_k \phi_{ik}^{\text{MIM}} + U_{\text{LRC}}, \quad (11)$$

where the first sum represents the contribution of the particles in the simulation box, the second sum corresponds to the contribution of the minimum image particles from outside of the box, and the third term is a correction of the long-range interactions using mean-density approximation  $U_{\text{LRC}} = 2\pi\rho \int_{r_c}^{\infty} r^2 \phi(r) dr$  (for LJ equation (2)). The essential difference between the traditional approach (in which the second term disappears) and the proposed method lies in the fact that, during the sampling of the box in the traditional approach, i.e. with using the mean-density correction, one loses information on the spatial arrangement of the minimum image particles remaining outside the simulation box. In the proposed method, this contribution of the crystal symmetry to the elastic energy during fluctuations of the simulation box is taken into account, resulting in an increased accuracy of the result.

As it will be shown further, the MIM calculations allow one to obtain quite accurate values of the elastic constants (which differ by only a few percent from those in the thermodynamic limit) by simulating relatively small systems (of 100–200 particles). It is worth noticing that to achieve similar accuracy results by only increasing the size of the simulated system and extrapolating the thermodynamic limit, the required computational time is larger.

### 3.3. Simulation details

For evaluation of the elastic constants the simulations in the NVT and NPT ensembles were performed for both traditional MC and MC with MIM. The samples of  $N = 4n^3$  particles were simulated, where  $n = 2, 3, 4, 5, 6, 7, 8, 10$  in the canonical ensemble and  $n = 3, 4, 5, 6, 7, 8$  in the NPT ensemble. In the MC simulations, two kinds of trial motions were used. The first, applied both in the NPT and NVT simulations, concerned changes of the particle positions and its acceptance ratio was kept close to 40%. The second kind of the motions, performed in the NPT simulations only, corresponded to changes of the components of the symmetric box matrix; it was tried about  $N^{1/2}$  times less frequently than the particle motions. These box motions determined the size and the shape

of the box and their acceptance ratio was close to 30%. In the NVT ensemble typical length of the run was equal to  $5 \times 10^5$  cycles (trial steps per particle) for all system sizes after equilibration  $\times 10^4$ . In the NPT simulations the lengths of the runs depended on the size of the system. For both traditional MC and MC with MIM in the NPT ensemble, the typical lengths of the runs were equal to  $3 \times 10^6$  cycles for  $n = 3$ ,  $5 \times 10^6$  cycles for  $n = 4$ ,  $10^7$  cycles for  $n = 5$ ,  $2 \times 10^7$  cycles for  $n = 6$ ,  $3 \times 10^7$  cycles for  $n = 7$ , and  $4 \times 10^7$  cycles for  $n = 8$ , after equilibration.

## 4. Results and discussion

### 4.1. Nearest-neighbor LJ model vs model with cut LJ potential

As it was mentioned in the Introduction, calculations of elastic constants of the LJnn model as the reference system are often used in the literature for various purposes. The present calculations are in excellent agreement with the literature results (see Fig. 1). Moreover, as one can see in Fig. 1, all the elastic constants  $C_{11}$ ,  $C_{12}$  and  $C_{44}$  obtained by different methods and by different authors are in a perfect harmony with each other (the lower line and points in Fig. 1). This cannot be said about the simulation results for the system of particles interacting through the full LJ potential, i.e. taking into account further (than the nearest) neighbors (the upper line and points in Fig. 1). An ample spread of results that may be associated with different values of the cut-off potential is observed.

To illustrate this, one can see that the elastic constants  $C_{11}$  and  $C_{44}$  obtained by Squire, Holt, and Hoover [1], despite large calculation errors are not in good agreement for  $T^* = 0.5$  with the results obtained by Quesnel, Rimai, and DeMejo [19]. The upper line and dots show the results of calculations of the elastic constants in the NVT ensemble for  $N = 108$  where the long-range interactions are taken into account using the MIM. In this case,  $r_c$  for calculating the elastic constants in the fluctuation formula Eq. (6) was about  $7\sigma$ , which allows one to take into consideration the most essential long-range interactions for the LJ potential and the (fcc) crystalline structure. This will be seen even clearer in the next section during the discussion of the results of calculations of the elastic constants of the LJ system in the thermodynamic limit. Now, let us analyze the cutoff radius influence on the elastic constants. In Fig. 2 the potential energy, pressure, and elastic constants are shown as functions of the cut-off radius of the LJ potential. One can see that the energy and pressure for the  $r_c > 4\sigma$  are nearly constant and are close to the thermodynamic limit values. For additional validation of the present calculations, a comparison of the present results with the literature is shown in Table 1. As one can see, the energy and pressure are in perfect compliance. However in the case of elastic constants (see Fig. 2), the impact of further neighborhood is much larger than for the energy and pressure. Moreover, the lack of the long-range corrections leads to incorrect results. Fig. 2 also shows that the convergence of elastic constants to the thermodynamic limit values is much slower than for the energy and pressure. Hence, they require much larger values of the cut-off radius, at least  $r_c > 6\sigma$ .

### 4.2. Elastic constants in the thermodynamic limit ( $N \rightarrow \infty$ )

The elastic constants of the system of particles interacting via the LJ potential were determined in two thermodynamic ensembles (NVT and NPT). To determine the elastic constants in the NVT ensemble, the fluctuation formula (6) was applied. For calculation of the elastic constants in the thermodynamic limit three different approaches were used: (i) a spherical truncation ( $r_c$  MC), (ii) all particles in the simulation box (box MC), (iii) the minimum image method (MIM MC). In the first approach the elastic constants were determined by using the fluctuation formula which was

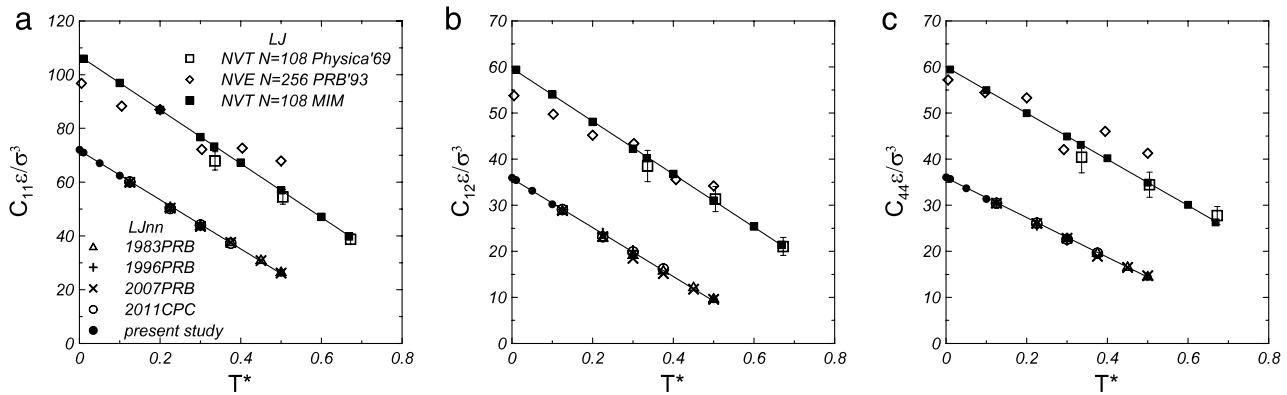


**Fig. 1.** Elastic constants as functions of temperature ( $T^* = kT/\epsilon$  where  $k$  is Boltzmann's constant and  $T$  is the temperature). The bottom lines and points on (a), (b), and (c) represent the LJnn model. The top lines and points correspond to the systems of particles interacting via cut LJ potential. Linear fits are used to determine the elastic constants at  $T \rightarrow 0$ .

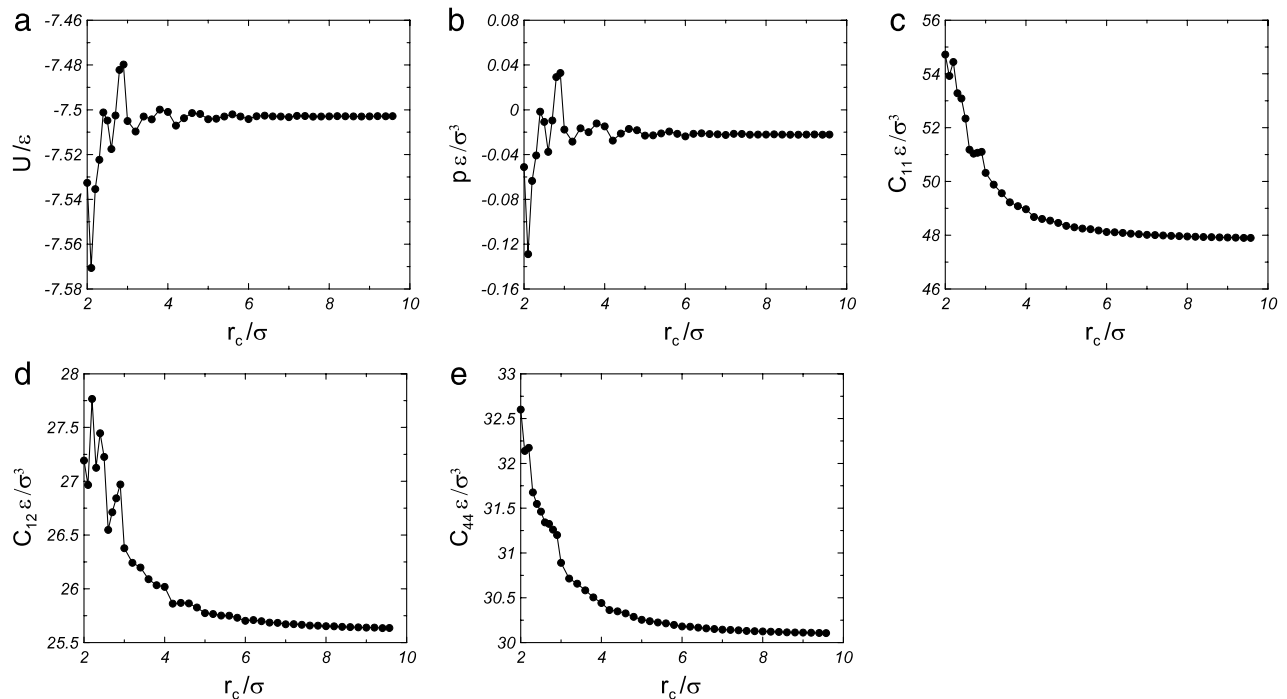


**Fig. 2.** Energy (a), pressure (b), and elastic constants (c–d) as functions of cut-off radius obtained by MC simulations with the MIM of the systems of 256 particles interacting via cut LJ potential at  $T^* = 0.6$  and  $\rho^* = 0.9852$ . Here, the simulations in the canonical ensemble are performed by the standard (Metropolis) Monte Carlo scheme (with  $r_c = L/2$  where  $L$  is the simulation box length) and MIM with different  $r_c$  used only for calculations of energy, pressure and elastic moduli. The lines are just to guide the eye.

**Table 1**

MC simulation results in the canonical ensemble for  $N = 500$  particles interacting via LJ potential. Comparison of the energy and pressure obtained at this work for the system at different thermodynamic states with the literature results [20].

$\rho^*$	$T^*$	$U^*$	$U_{ref}^*$	$p^*$	$p_{ref}^*$	$r_c/\sigma$
0.6	1.0	−4.220(5)	−4.228(6)	−0.266(8)	−0.269(9)	4.71
0.7	1.0	−4.889(1)	−4.890(2)	0.030(8)	0.019(10)	4.47
0.8	1.0	−5.535(3)	−5.533(1)	1.026(22)	1.03(1)	4.27
0.9	2.0	−5.029(2)	−5.030(4)	9.11(2)	9.09(2)	4.11

applied only for the particles being within the sphere diameter  $r_c$ . In this case  $r_c$  was chosen to be equal to half of the simulation box ( $L/2$ ). A series of MC simulations with increasing size of the system were performed. Based on obtained results, the elastic constants in the thermodynamic limit have been determined using extrapolation  $N \rightarrow \infty$  for results of calculations of the elastic constants for different system sizes. The results for this approach are shown in Fig. 3 by circles and the dotted line. One can see there a strong dependence of the elastic constants on the size of the system.

In the second approach (*box* MC), the fluctuation formula was applied to all the particles in the simulation box (squares and dashed line, see Fig. 3). One can see there a significant improvement in the convergence to the thermodynamic limit. It is associated with taking into consideration a larger number of particles – all the particles in the box of periodicity.

In the third case (*MIM* MC), in calculation of the elastic constants by the fluctuation formula was used the method of the minimum image which takes into account all of the particles in the

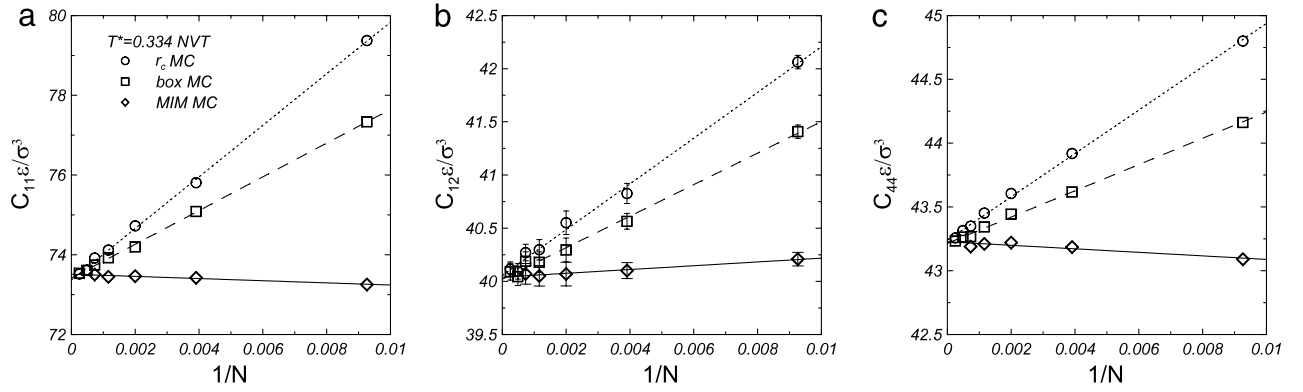


**Fig. 3.** Results of MC simulations in the NVT ensemble. Elastic constants of LJ system as a function  $1/N$  where  $N$  is the number of particles in the simulation cell. The linear fits were used to determine the values of elastic constants in the thermodynamic limit,  $N \rightarrow \infty$ .

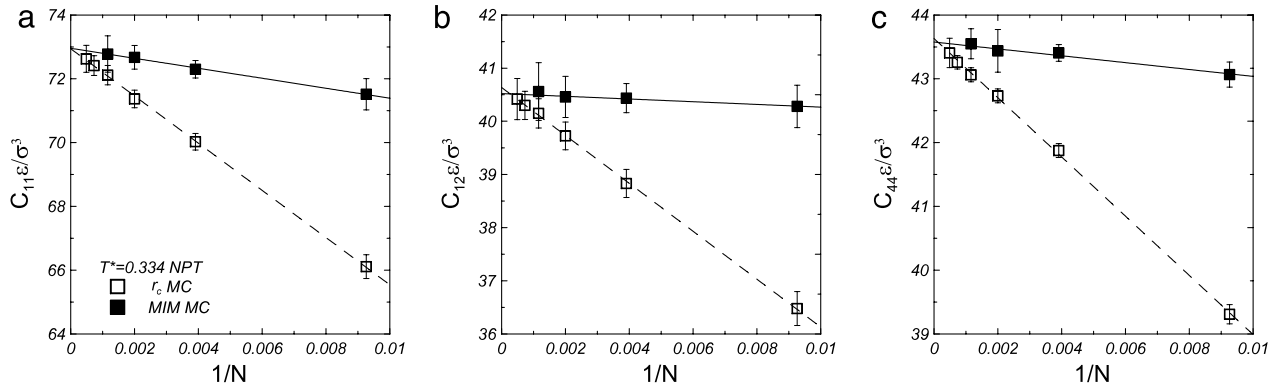


**Fig. 4.** Results of MC simulations in the NPT ensemble. Elastic constants of LJ system as a function  $1/N$  where  $N$  is the number of particles in the simulation cell. The linear fits were used to determine the values of elastic constants in the thermodynamic limit,  $N \rightarrow \infty$ .

box of periodicity and its nearest images. In Fig. 3, the obtained results are presented by the black dots and the solid line of extrapolation determines the value of elastic constant in the thermodynamic limit. Here, one can see very weak dependence of the values of the elastic constants from the size of the system. This allows one for using very small systems, of order of 100 particles, to get the results that differ by only a few percent from the values of elastic constant in the thermodynamic limit.

The MC simulations in the NPT ensemble were performed in two versions. In both cases, the elastic constants were determined by the modified Parrinello–Rahman method [29,30]. In the first case, the simulation was performed using the Metropolis sampling (scheme) for particles in a sphere of diameter  $r_c = L/2$  and using the standard amendments to the energy (2). The results of these simulations are shown in Fig. 4 by open squares and the thermodynamic limit was determined by extrapolation (dashed line). Here, as well as in the case of canonical ensemble (open circles in Fig. 3), one can observe a strong dependence of the elastic constants on the size of the system. In the second case, using the method of minimum images in simulations (full black squares in Fig. 4) provides negligible dependence of elastic constants on the system size. It is the result of good approximation of the contribution of the part of energy which simultaneously takes into account the symmetry of the crystal and the long-range interactions. The main difference between the first and the second approach is that in the first case the amendment to the energy based on the mean density approximation leads to the poor estimation of the part of energy which is related to deformation of the simulation box when changing the components of the box matrix. In the second case, using the MIM, this disadvantage is eliminated by consideration of the images of the particles present in the box of periodicity. This results in the correct estimation of both the contributions to the energy (strictly

speaking the enthalpy) of the system: (i) the deformation of simulation box and (ii) the long-range interactions.

In Table 2, there are shown the results of calculations of elastic constants for the different temperatures at zero pressure for systems of  $N = 32$  and 108, using the MIM and the elastic constants of the thermodynamic limit. Analyzing the results contained in Table 2 it can be seen that using the MIM for calculating the elastic constants in a very small system consisting of only  $N = 32$  particles provides an estimate of their values that differ from those at the thermodynamic limit by about 6%, and for  $N = 108$  that difference less than 0.8%.

#### 4.3. Efficiency of the methods

Comparison of the program execution times of the traditional MC simulations in the NVT ensemble and the MC simulations with MIM are shown in Fig. 5. In both cases the execution times increase with the number of particles as the square of the number of particles in the system. In Fig. 5 one can see that the calculations of the elastic constants for the same size of the system take approximately 10 times longer for simulations using the MIM than the traditional approach. On the other hand, it can be seen that the effective number of particles considered in the case of the minimum image method compared to the conventional method is 27 times greater, and the simulation time increases only 10-fold. This means that in the simulation with  $N = 108$  using MIM, the calculations of elastic constants are performed for 2916 particles. One should stress that the simulation of a system of such a size by the traditional method would require about 60 times longer time (full black circles in Fig. 5). There are other arguments in favor of the MIM: (i) traditional approach for long-range interactions (such as LJ) fails, and (ii) only the use of large systems allows



**Table 2**  
MC simulation results in the canonical ensemble. Comparison of the elastic constants in the thermodynamical limit with results obtained using the MIM for the systems consisting of  $N = 32$  and 108 particles.

$T^*$	$\rho^*$	$C_{11}^*$ $N \rightarrow \infty$	$C_{11}^*$ $N = 108$	$C_{11}^*$ $N = 32$	$C_{12}$ $N \rightarrow \infty$	$C_{12}$ $N = 108$	$C_{12}$ $N = 32$	$C_{44}$ $N \rightarrow \infty$	$C_{44}$ $N = 108$	$C_{44}$ $N = 32$
0.01	1.0909	105.80(5)	105.94(4)	103.8(1)	59.36(4)	59.40(3)	60.3(1)	59.47(2)	59.46(1)	58.38(5)
0.1	1.078	97.0(1)	96.93(9)	95.6(1)	54.0(1)	54.03(8)	54.4(1)	55.04(4)	54.98(3)	54.11(5)
0.2	1.0625	87.1(2)	86.85(17)	85.3(2)	48.1(2)	48.09(15)	48.5(2)	50.08(5)	49.98(5)	49.0(1)
0.3	1.0455	77.1(3)	76.8(2)	75.1(2)	42.1(3)	42.26(18)	42.9(2)	45.1(1)	44.92(9)	43.9(1)
0.4	1.028	67.8(4)	67.3(3)	65.4(2)	36.7(3)	36.8(3)	37.4(2)	40.3(1)	40.2(1)	39.2(1)
0.5	1.0067	57.2(5)	57.0(4)	54.8(4)	30.6(4)	31.0(3)	31.6(3)	35.0(2)	34.9(1)	34.0(2)
0.6	0.9852	47.6(5)	47.1(5)	45.4(6)	25.3(4)	25.4(5)	26.6(5)	30.2(2)	30.1(1)	29.3(2)
0.668	0.9667	40.1(6)	39.8(5)	37.6(5)	21.1(5)	21.4(4)	22.2(5)	26.3(2)	26.3(2)	25.6(2)

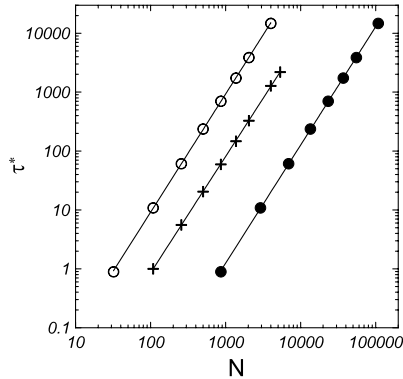


**Fig. 5.** Dependence of the relative program execution time on the number of particles in the system. The relative program execution time is defined as  $\tau^* = \tau/\tau_{108}$ , where  $\tau$  is the program execution time and  $\tau_{108}$  is its value for  $N = 108$  of traditional MC simulation in the NVT ensemble. Crosses correspond to MC simulations in the NVT ensemble. Circles represent the simulations using the MIM. Full black circles show the dependence of the relative execution time of the program from the effective number of particles considered in calculations of the elastic constants using the MIM.

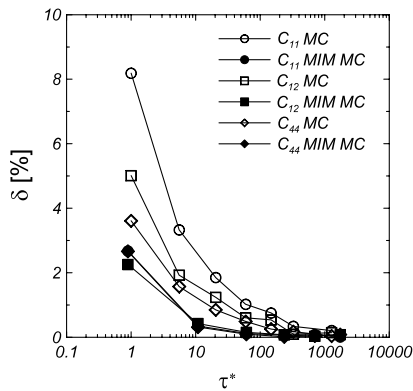


**Fig. 6.** Dependence of the relative error ( $\delta = \left| \frac{C_{ij}(N \rightarrow \infty) - C_{ij}}{C_{ij}(N \rightarrow \infty)} \right| \times 100\%$ ) on the relative program execution time.  $C_{ij}(N \rightarrow \infty)$  is the value of the elastic constant in the thermodynamical limit. The comparison has been made for simulation results at  $T^* = 0.334$  and  $\rho^* = 1.039$ . The lines are just a guide to the eye.

to obtain good results, whereas (iii) the method of the minimum image is very easy to implement, and for small systems (non time-consuming calculations) gives results that are very close to the values of elastic constants in the thermodynamical limit. This clearly shows the advantage of the MIM for the calculation of elastic constants of systems with long-range interactions. Therefore the use of this method is desirable in calculations where – for various reasons, e.g., complexity of the system – it is not possible to carry out calculations for large systems and the inclusion of long-range interactions is necessary. The final argument in favor of the minimum image method is the fact that to obtain the results of the same accuracy one needs less computational time when using MC

with MIM than in the case of the traditional MC simulations, see Fig. 6. In that figure, one can see that at identical program execution times, the relative error is smaller for MC with MIM than for the standard MC simulations.

## 5. Summary and conclusions

The elastic constants of the LJ system in the thermodynamic limit  $N \rightarrow \infty$  have been calculated in the NVT and NPT ensembles using the standard MC simulations and using the MC simulation with the MIM. The proposed method allows one to obtain correct values of the constants of elasticity in both the NVT and NPT ensembles. Instead of using the mean-density approximation the simple and effective method of minimum image is proposed, which taking into account the long-range interactions better reproduces the symmetry of the studied solid. Simply, for particles moving in the simulation box, one needs to take into account the terms coming from interaction between the next-nearest-neighbor images of the particles. Here, it should be noticed also that to achieve the same relative error of the elastic constants using the MC simulation with MIM, shorter times of calculation are required than using the standard MC scheme.

The main advantage of simulations with MIM in the NVT ensemble is its fast convergence – short equilibration time and rather quick simulations are sufficient for evaluating the elastic properties. The main disadvantage is that the fluctuation formula is typically used when the interaction potential is spherically-symmetric; otherwise a use of the fluctuation formula is difficult.

The advantage of simulations with MIM in the NPT ensemble is that one can explore a broad class of potentials, which do not need to be spherically symmetric. The disadvantage is slow convergence – very long runs must be performed for large systems. However, for small systems (about one hundred of particles) using the MIM a reasonable result can be quickly obtained, that differs by less than 1% (for the LJ system) from that in the thermodynamical limit.

It is worth noting that some test simulations were also carried out using molecular dynamics (MD) in the NVT ensemble with MIM. Simulation results obtained using the MC and MD methods were in a good agreement with each other.

## Acknowledgments

KVT would like to thank Dr. Bartłomiej Kowalczyk (Northwestern University) for kindly reading and commenting on the manuscript. This work was supported by the Grant No. N N202 261438 of the Polish Ministry of Science and Higher Education (MNiSW) and partially by the Polish National Science Center grant DEC-2012/05/B/ST3/03255. Part of the calculations was performed at the Poznań Computing and Networking Center (PCSS).

## References

- [1] D.R. Squire, A.C. Holt, W.G. Hoover, *Physica* 42 (1968) 388.
- [2] M. Parrinello, A. Rahman, *J. Chem. Phys.* 76 (1982) 2662.

- [3] M. Sprik, R.W. Impey, M.L. Klein, *Phys. Rev. B* 29 (1984) 4368.
- [4] J.R. Ray, A. Rahman, *J. Chem. Phys.* 80 (1984) 4423.
- [5] J.R. Ray, A. Rahman, *J. Chem. Phys.* 82 (1985) 4243.
- [6] A.A. Gusev, M.M. Zehnder, U.W. Suter, *Phys. Rev. B* 54 (1996) 1.
- [7] Z. Zhou, B. Joos, *Phys. Rev. B* 54 (1996) 3841.
- [8] Z. Cui, Y. Sun, J. Li, J. Qu, *Phys. Rev. B* 75 (2007) 214101.
- [9] J. Li, Z. Cui, F. Zeng, *Comput. Phys. Comm.* 182 (2011) 1447.
- [10] Y. Zhen, C. Chu, *Comput. Phys. Comm.* 183 (2012) 261.
- [11] E. Voyiatzis, *Comput. Phys. Comm.* 184 (2013) 27.
- [12] J.-P. Hansen, I.R. McDonald, *Theory of Simple Liquids*, Academic Press, Amsterdam, 2006.
- [13] M.P. Allen, D.J. Tildesley, *Computer Simulation of Liquids*, Clarendon Press, Oxford, 1987.
- [14] E.R. Cowley, *Phys. Rev. B* 28 (1983) 3160.
- [15] J.R. Ray, M.C. Moody, A. Rahman, *Phys. Rev. B* 33 (1986) 895.
- [16] M. Li, L. Johnson, *Phys. Rev. B* 46 (1992) 5237.
- [17] K.V. Workum, J.J. de Pablo, *Phys. Rev. E* 67 (2003) 011505.
- [18] W.G. Hoover, A.C. Holt, D.R. Squire, *Physica* 44 (1969) 437.
- [19] D.J. Quesnel, D.S. Rimai, L.P. DeMejo, *Phys. Rev. B* 48 (1993) 6795.
- [20] J.K. Johnson, J.A. Zollweg, K.E. Gubbins, *Mol. Phys.* 78 (1993) 591.
- [21] J.Q. Broughton, G.H. Gilmer, *J. Chem. Phys.* 79 (1983) 5095.
- [22] P. Ewald, *Ann. Phys.* 64 (1921) 253.
- [23] S.W. de Leeuw, J.W. Perram, E.R. Smith, *Proc. R. Soc. Lond. Ser. A* 373 (1980) 27.
- [24] D.M. Heyes, *J. Chem. Phys.* 74 (1981) 1924.
- [25] R.W. Hockney, J.W. Eastwood, *Computer Simulation Using Particles*, McGraw-Hill, New York, 1981.
- [26] A.C. Ladd, *Mol. Phys.* 33 (1977) 1039.
- [27] A.C. Ladd, *Mol. Phys.* 36 (1978) 463.
- [28] L.D. Landau, E.M. Lifshits, *Theory of Elasticity*, third ed., Pergamon Press, Oxford, 1993.
- [29] K.W. Wojciechowski, K.V. Tretiakov, *Comput. Phys. Comm.* 121–122 (1999) 528.
- [30] K.W. Wojciechowski, K.V. Tretiakov, A.C. Brańka, M. Kowalik, *J. Chem. Phys.* 119 (2003) 939–946.
- [31] Q.W. Metropolis, M.N. Metropolis, A.H. Rosenbluth, A.H. Teller, E. Teller, *J. Chem. Phys.* 21 (1953) 1087.